BOND GRAPH MODELING OF BRAKE-BY-WIRE ACTUATORS ON A ONE-WHEEL VEHICLE MODEL

Ehsan Arasteh
Francis Assadian

University of California, Davis
One Shields Avenue, Davis, California, USA
earasteh@ucdavis.edu, fassadian@ucdavis.edu

ABSTRACT

This paper discusses the modeling and simulation of three different brake-by-wire actuators utilizing bond graph method. The brakes studied include a hydraulic brake with a modulated pressure (Electro-Hydraulic) and two different Electro-Mechanical Brake configurations that use electric motors to move the caliper. After modeling the actuators with the use of bond graphs, a one-wheel model is used to compare the actuators (in terms of stopping distance) and the effort of the actuators (energy spent to stop). Finally, the electro-hydraulic brake was optimized using the parameters chosen based on the equations derived from the bond graphs.

Keywords: : Brake-by-wire, Bond Graph, Electro-Hydraulic Brake, Electromechanical Brake, Electronic Wedge Brake, Simulation

1 INTRODUCTION

X-By-Wire technologies are the future of the automotive industry due to the increasing demand for electrification and fuel efficiency. Their electronic architectures and interface also make them great candidates for autonomous and hybrid electric/electric vehicles. Among all the necessary by-wire technologies, brake-by-wire systems are a priority due to their safety-critical nature in a vehicle [1][2].

Brake-by-wire systems can reduce component weight and allow the actuators to consume energy only when required by blending both regenerative braking and friction braking. This can minimize fuel consumption and CO_2 emissions. Using sensors and control methods, caliper drag can be eliminated by making brake-by-wire technology even more energy efficient. Individual wheel braking and faster activation time can be combined with the vehicle's ECS system to make the vehicle safer. The reliability of new actuators and the risk and cost associated with deploying new brake technologies are the main hurdles of brake-by-wire systems becoming a popular choice in automotive manufacturers [3][4].

Brake systems are categorized into wet and dry brakes. Wet brakes employ fluids for their operation, and dry brakes are usually purely mechanical systems. Electro-hydraulic brake systems are a type of wet brakes where their pressure is modulated using pressure modulators that can be controlled electronically. The pressure source can be packaged in one centralized location for all four wheels like Bosch's first electro-hydraulic brake system [5], or it can be local to each wheel like MK C-1 from Continental [6] (local Electro-hydraulic brakes).

Dry brakes can also be realized in a few different configurations. There is an electro-mechanical brake that utilizes a small motor, planetary gear set, and a roller screw actuator to move the brake pad [7]–[13]. However, this type of brake requires a 42 Volt motor to operate and consumes a lot of energy [3]. Electronic wedge brakes, on the other hand, uses a wedge mechanism to create a system that draws the wedge pad inside the brake; therefore, requiring less energy to operate [13]–[21]. Vienna Engineering has also developed a

similar system that uses a crank-shaft mechanism to reduce the complexity of reduction gears and roller screw actuator [22]–[25].

In this paper, we have chosen to study and compare electro-hydraulic, electro-mechanical, and electronic wedge brakes. In the first section, the bond graphs and equations of the brake models are presented. In the second section, the control strategy is explained. Finally, in the simulation results section, we present all the comparisons and simulation results for the brake systems under different conditions.

2 SYSTEM MODELING

In this section, we discuss the schematics, bond graphs, and the state equations derived from the bond graphs for each brake system. All the actuator models include a one-wheel vehicle model that is represented in Figure 1. It includes a moving wheel with rotational inertia connected to a point mass. This simple dynamic model aids the preliminary studies of brake actuators and algorithms (such as ABS and TCS) and is easy to implement on a test rig [25]–[29]. The bond graph of this model is included in Figure 2.

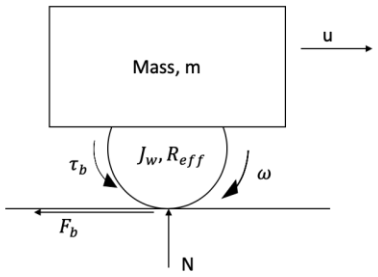

Figure 1: Schematic of a One-Wheel Model

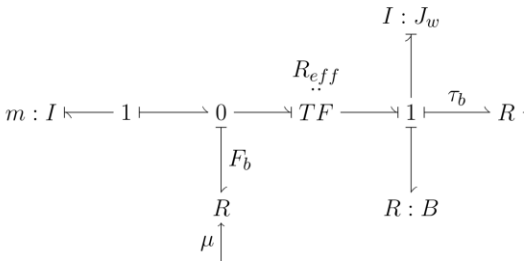

Figure 2 : Bond Graph of one-wheel vehicle model

2.1.1 State Equations

State equations for this model are as follows

$$\dot{\boldsymbol{p}}_{\boldsymbol{w}} = \boldsymbol{J_w}\dot{\boldsymbol{\omega}} = \boldsymbol{F_b R_{eff}} - \boldsymbol{\tau_b} - \boldsymbol{B\omega} \quad (1)$$

$$\dot{\boldsymbol{p}}_{\boldsymbol{u}} = \boldsymbol{m}\dot{\boldsymbol{u}} = -\boldsymbol{F_b} \quad (2)$$

Where u is forward velocity, ω is wheel angular velocity, τ_b is braking torque, F_b is braking force, N is the normal force, B is bearing friction coefficient, R_{eff} is effective wheel radius, $\dot{p}_\omega$ is the angular momentum of the wheel, and $\dot{p}_u$ is the vehicle's momentum. For the braking force modeling, the Burckhardt tire model is chosen in which the coefficient of friction (μ) is a function of the longitudinal slip (λ) (Equation 4), and the longitudinal slip during a skid is defined in Equation 3 [30][31].

$$\boldsymbol{\lambda} = \frac{\boldsymbol{u} - \boldsymbol{\omega R_{eff}}}{|\boldsymbol{u}|} \quad (3)$$

$$\boldsymbol{F_b} = \boldsymbol{\mu(\lambda)} \cdot \boldsymbol{N} = \left[\boldsymbol{c_1}\left(\boldsymbol{1} - \boldsymbol{e}^{-\boldsymbol{c_2\lambda}}\right) - \boldsymbol{c_3\lambda}\right] \cdot \boldsymbol{N} \quad (4)$$

The state equations describing the one-wheel model will always be present in all brake type models since the vehicle model will stay the same.

2.2 Electro-Hydraulic Brake Actuator

The schematic of an electro-hydraulic brake (EHB) actuator is presented in Figure 3. It includes a hydraulic pipe that carries the hydraulic fluid with the pressure input (P_{in}) to a cylinder chamber, which in turn changes this pressure into the movement of the brake pad. Therefore, the brake pad movement results in stopping the brake disk from moving [32].

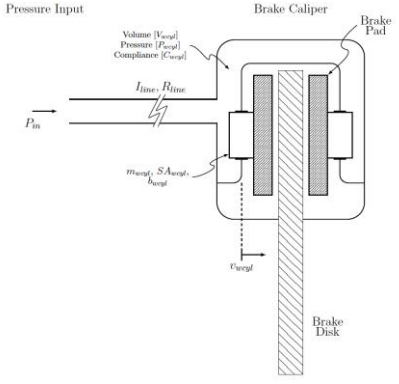

Figure 3: Schematic of an EHB actuator [32]

2.2.1 Bond Graph Model

The bond graph model is derived based on the schematic in Figure 3 and the bond graph in Figure 2. The input is modulated pressure, and this pressure is an input to the hydraulic line, where, by using a transformer, it results in the brake pad movement (the pressure reservoir, value, and the motor that modulates the value are not included in the model and can be added later on). The interaction between the brake pad and the wheel is modeled with a stiffness (k_{cal}). Brake torque is also modeled as a modulated resistance which changes with the displacement of the brake pad. The modulated resistance formula is given by Equation (9) which describes the brake torque as a function of caliper distance to the rotor (the normal caliper force is translated to the torque).

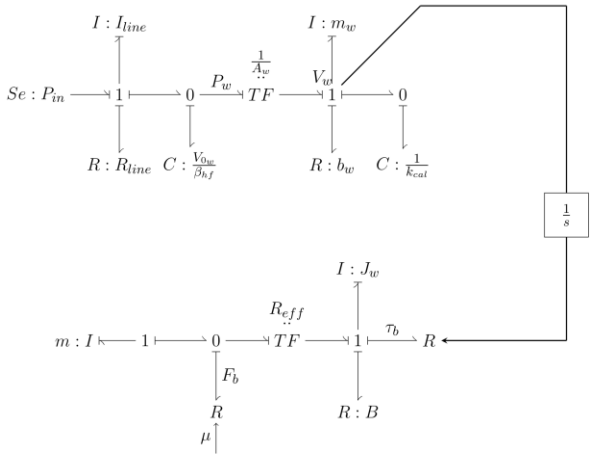

Figure 4: Bond graph of an EHB actuator

2.2.2 State Equations

State equations are derived based on the bond graph in Figure 3.

$$\dot{p}_{\text{line}} = P_{\text{in}} - R_{\text{line}} \frac{p_{\text{line}}}{I_{\text{line}}} - q_w \frac{\beta_{hf}}{V_{0_w}} \quad (5)$$

$$\dot{q}_w = \frac{p_{\text{line}}}{I_{\text{line}}} - A_w \frac{p_w}{m_w} \quad (6)$$

$$\dot{p}_w = A_w q_w \frac{\beta_{hf}}{V_{0_w}} - b_w \frac{p_w}{m_w} - q_{cal} k_{cal} \quad (7)$$

$$\dot{q}_{cal} = \frac{p_w}{m_w} \quad (8)$$

Where
$R_{line}, p_{line}, I_{line}, \beta_{hf}, V_{0_w}, A_w, p_w, V_w, and\ q_{cal}$
are hydraulic line resistance, hydraulic line pressure, line inertia, bulk modulus, the volume of cylinder chamber, the surface area of the piston, pressure on the back of the brake pad, velocity of the brake pad, and brake pad position, respectively.

The brake torque is calculated using Equations 9 as follows,

$$\tau_b = \begin{cases} 2\mu_{cal} r_{eff} k_{cal} (x_{cal} - x_0), & \text{if } x_{cal} \geq x_0 \\ 0, & \text{otherwise} \end{cases} \quad (9)$$

Where $\mu_{cal}, r_{eff}, x_{cal}, and\ x_0$ are brake friction coefficient between the pad and the wheel, brake pad effective radius, brake pad position (same as q_{cal}), and brake clearance, respectively.

Equations 5-9 along with Equations 1-4 present the state equations for this brake system [32].

2.3 Electro-Mechanical Brake Actuator

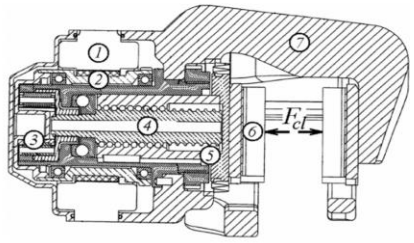

Figure 5 Cross-section of an Electro-Mechanical Brake System, a patent by PRB Australia Pty Ltd.[33]

Figure 5 shows a schematic of an electro-mechanical brake actuator. Numbers 1-7 show the location of the motor stator, motor rotor, planetary gear set, ball screw, piston, brake pad, and floating caliper to oppose the brake pad. In this actuator, the motor's rotational motion becomes the brake pad's movement through one (or more) planetary gear sets and a ball screw mechanism. This movement will then create a clamping force noted at F_{cl} in Figure 5 [10][33].

2.3.1 Bond Graph Model

Figure 6 illustrates the bond graph model for an electromechanical brake actuator. The input to the system is voltage (V_{in}) to the motor. The motor includes an inductance (L_m) and a resistance (R_m). The motor's current is proportional to a torque on the shaft and this proportionality is modeled by a gyrator (with K_t representing the motor constant). The shaft has a rotational inertia (J_{shaft}). The resistance that exists inside the planetary gear set, the ball-screw mechanism, and the motor shaft are lumped together and modeled by an R-element. This resistance element is explained more in the next section. The transformer is then used for the planetary gear set ratio (N_{pl}) and the ball-screw mechanism lead ratio (N_{Screw}). And finally, the interaction between the brake pad and the wheel is modeled with a stiffness similar to the one in the electro-hydraulic brake system's bond graph (K_{cal}).

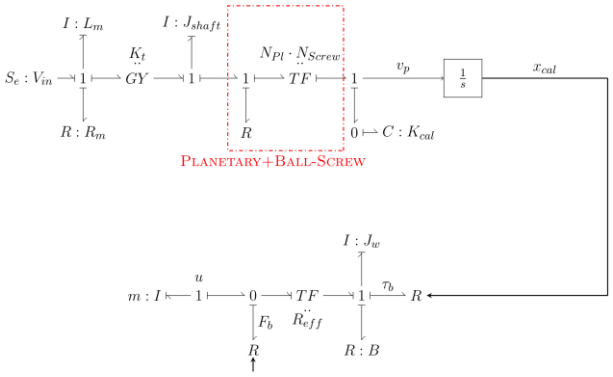

Figure 6: Bond graph of an electro-mechanical brake system

2.3.2 State Equations

Based on the bond graphs in Figure 6, the state equations are presented in Equations 10-12. Also, the brake torque is calculated similar to the electro-hydraulic system using Equation 9. As shown in the Equations (11) and (12), it is assumed that the ball-screw in the EMB model is back-drivable.

$$\dot{I}_m = \frac{1}{L_m} \cdot (V_{in} - R_m \cdot I_m - K_t \cdot \omega_m) \tag{10}$$

$$\dot{\omega}_m = \frac{1}{J_{\text{shaft}}} \cdot \{\mathrm{K_t} \cdot I_m - \tau_f - N_p \cdot N_s \cdot \mathrm{K_{cal}} \cdot max(x_{cal} - x_0, 0)\} \tag{11}$$

$$\dot{X}_{cal} = N_s \cdot N_p \cdot \omega_m \tag{12}$$

The lumped friction torque (τ_f) is modeled using Karnopp friction [34] with the Coulomb friction torque (τ_c) and maximum stiction torque (τ_s) having an affine relationship with the clamping force (F_{cl}). The area around zero of the motor rotational velocity is given by $d\omega$, and ω_m is the motor's rotational velocity and τ_{pl_0} is the friction torque when the shaft is not moving. C, G, and T_s are constants that can be acquired using experimental results [10][34].

$$\tau_f = \begin{cases} \tau_c \cdot \text{sign}\,(\omega_m) + b_v \cdot \omega_m & |\omega_m| \geq \mathrm{d}\omega \\ min\left(|\tau_{pl_0}|, |\tau_s|\right) \cdot \text{sign}\,(\tau_{pl_0}) & \text{else} \end{cases} \tag{13}$$

$$\tau_c = C + G \cdot F_{cl} \tag{14}$$

$$\tau_s = T_s + G \cdot F_{cl} \tag{15}$$

2.4 Electronic Wedge Brake Actuator

Figure 7 shows the cross-section of an electronic-wedge brake actuator. The difference between this actuator and the electro-mechanical brake system is the slope shape of the caliper and the wedge that can create a self-reinforcing force drawing the wedge inside (wheel's movement draws the wedge inside, F_{aux}); thus, requiring less force from the electric motor to stop the wheel.

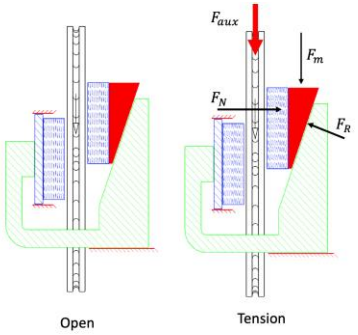

Figure 7: Principle of how electronic wedge brake actuator works [14]

Based on Figure 7, we can draw a schematic for the wedge and the caliper as shown in Figure 8. The motor's rotational velocity is being translated through a roller screw actuator to a linear force on

the wedge. The motor shaft's axial stiffness and resistance are also added to the system.

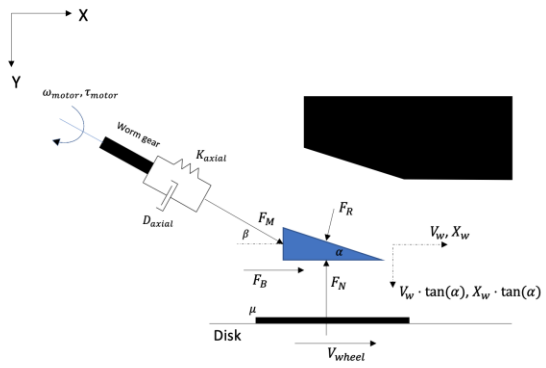

Figure 8: Schematic of the wedge in the electronic wedge brake [15]

If we write the force equations for the wedge brake, we can get

X-direction:

$$m_w \dot{V}_w = F_M \cos\beta + \mu F_N - F_R \sin\alpha \qquad (16)$$

Y-direction:

$$m_w \dot{V}_w \tan(\alpha) = F_M \sin\beta - F_N + F_R \cos\alpha \qquad (17)$$

And for the disk surface, we can write,

$$F_N = K_{\text{Cal}} \cdot X_w \tan(\alpha) \qquad (18)$$

Where $K_{caliper}$ represents the stiffness of the caliper itself (the area with the hashed line in Figure 7). A saturation for X_w values has been chosen to bound the maximum amount of normal forces. By rearranging Equations 16-18, we can remove the reaction force in the equations by substituting Equation 18 into 19. We have incorporated Equation 19 into the bond graph, in Figure 9, using 2 transformers.

$$\dot{V}_W = \frac{1}{m_W(1+\tan^2\alpha)} \cdot \qquad (19)$$
$$\left(\frac{1}{\cos\alpha} F_M + (\mu - \tan\alpha)\tan\alpha (K_{cal}) \cdot X_w\right)$$

2.4.1 Bond Graph Model

Figure 9 represents the bond graph of the electronic wedge brake. The input to the system is motor voltage. The electric motor section remains the same as discussed in the previous sections. The transformer includes the roller screw's lead ratio ($\frac{L}{2\pi}$) and the planetary gear set's gear ratio (N). For the sake of simplicity, we assume, $\alpha = \beta$. Therefore, the transformer gains T_1, T_2 and T_3 based on Equation 19, which will become Equations 20a-20c.

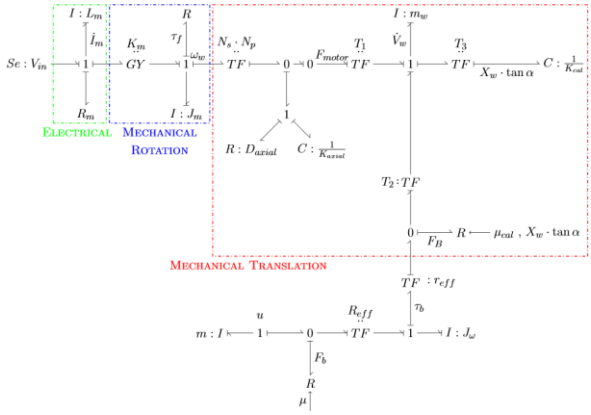

Figure 9: Bond graph of an electronic wedge brake

$$T_1 = \frac{1}{cos\,\alpha} \cdot \frac{1}{1+tan^2\,\alpha} = cos(\alpha) \qquad (20a)$$

$$T_2 = \frac{1}{1+tan^2\,\alpha} \qquad (20b)$$

$$T_3 = \frac{tan\,\alpha}{1+tan^2\,\alpha} \qquad (20c)$$

2.4.2 State Equations

Based on the bond graph, the equations of motion for the wedge brake are Equations 21-24. Brake torque is also calculated the same as other actuators.

$$\dot{I}_m = \frac{1}{L_m}(V_{in} - R_m I_m - K_m \omega_m) \qquad (21)$$

$$\dot{\omega}_m = \frac{1}{J_{\text{shaft}}}\Bigg(K_m I_m - \frac{L\cdot N}{2\pi}\Big[K_{ax} q_{ax} + D_{ax}\Big\{\frac{L\cdot N}{2\pi}\omega_m - \frac{1}{T_1}\cdot V_w\Big\}\Big]\Bigg) \qquad (22)$$

$$\dot{q}_{ax} = \frac{L\cdot N}{2\pi}\omega_m - \frac{1}{T_1} V_w \qquad (23)$$

$$\dot{V}_W = \frac{1}{m_w \cdot (1+\tan^2(\alpha))}\left\{\frac{1}{T_1}\left[K_{ax}q_{ax} + D_{ax}\left(\frac{L\cdot N}{2\pi}\omega_m - \frac{V_w}{T_1}\right)\right] - (\tan(\alpha)-\mu)\cdot K_{Cal}\cdot X_w \cdot \tan(\alpha)\right\} \quad (24)$$

Finally, Equation 25 shows how the brake torque (τ_b) is calculated. This is similar to Equation 9 including a saturation for the wedge displacement.

$$\tau_b = \begin{cases} 0, & \text{if } X_w\tan(\alpha) \le x_0 \\ 2\mu_{cal}r_{eff}k_{cal}(X_w - x_0)\cdot\tan(\alpha), & \text{if } x_0 \le X_w\tan(\alpha) \le x_{max} \\ 2\mu_{cal}r_{eff}k_{cal}(x_{max} - x_0)\cdot\tan(\alpha), & \text{if } X_w\tan(\alpha) \ge x_{max} \end{cases} \quad (25)$$

3 CONTROL STRATEGY

A smart actuator integrates sensors and low-level controllers all within the actuator. Controllers are designed to examine the performance of the three studied brakes as smart actuators. The controller design is based on the actuator dynamics without including the vehicle model. For each of the brake actuators, a transfer function was obtained using the linear equations of motion (all the nonlinearities in the frictions and caliper stiffness are linearized). And controllers in each case are designed using the Youla parameterization method [35]. This control strategy ensures internal stability, robustness, and reference tracking of the closed-loop system.

In the electro-hydraulic brake, the pressure is the input and the output is clamp force ($G_p = \frac{F_{cl}}{P_{in}}$). A controller was designed around the plant to follow a specific clamp force. In practice, we would need to either estimate the clamping force (or brake torque) or use a sensor to acquire this information [28].

For the electro-mechanical and electronic-wedge brakes, a cascaded control method is used. When the linearization of the system model for control design and the system includes severe nonlinearities, cascaded control strategy aids in less of a compromise between performance and robustness.

The block diagram for this control architecture is shown in Figure 10 [8], [10]. These controllers were also designed using the Youla parameterization method. In the cascaded control design, each inner closed-loop is a new open-loop to an outer controller, this is similar to sequential loop closure. In this case, for the first loop, the plant input is the motor's voltage and the output is the motor's current. For the second loop, the input is the motor's current and the output is the motor's angular velocity. Lastly, for the most outer loop, the input is the motor's angular velocity and the output is clamping force (the normal force that clamps the wheel).

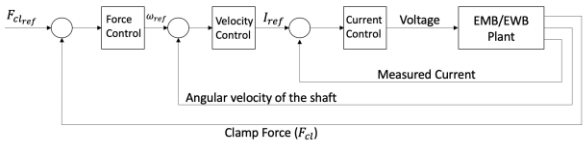

Figure 10: Cascaded Control Architecture for electro-mechanical and electronic wedge brakes

4 SIMULATION RESULTS

4.1 Open-Loop Response

The open-loop response of each brake system is shown in Figure 10. For the electro-hydraulic brake, a 4 MPa step pressure input is chosen to create a 10 kN steady-state clamp force which corresponds to around 900 N.m of brake torque. For the electro-mechanical and electronic wedge brakes, the input is chosen to be the motor's current instead of its voltage. This is assigned only to the inner loop as it was explained in the last section, which eliminates any possible effect that the motor dynamics has on the response. A step input of 5 A is chosen to create a 10 kN steady-state clamp force.

As shown in Figure 11, the electro-hydraulic brake is the fastest to reach the steady-state, and the electro-mechanical brake is the second-fastest. The fast response of the electro-hydraulic brake is one of its main advantages. Also, the transient responses are different, which reveals the dynamics of these brake actuators. They have under-damped, over-damped, and unstable (with saturation) responses, respectively.

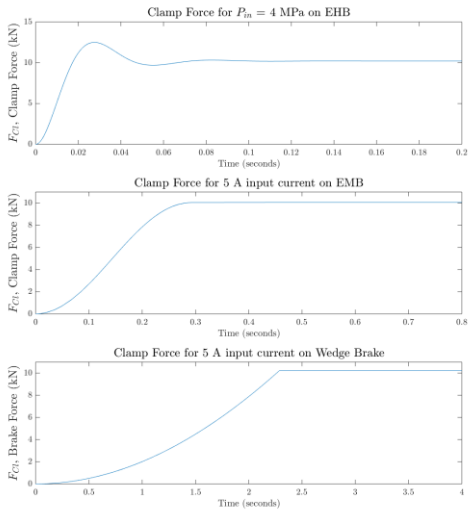

Figure 11: Open-Loop Response for each brake system

5 CLOSED-LOOP RESPONSE

Figure 12 shows the closed-loop response for a step clamp force as a reference. This clamping force is chosen to represent a nominal braking event without locking the wheel. The result of this brake torque on the vehicle is shown in Figure 13. All the brake actuators are designed to have close bandwidth. Therefore, as it is shown in Figure 12, all the actuators have very close settling time. As a result, the vehicle velocity and stopping distance would be identical for all the actuators. Figure 14 shows the wheel dissipated power by each actuator to perform the closed-loop tests which are related to the kinetic energy of the wheel. Since the brake torque references are the same and the controllers are designed around the same frequencies, the result would be close to each other. The electro-hydraulic brake has the smallest wheel dissipation peak, followed by the electro-mechanical and electronic wedge brake. This peak is directly related to the overshoot in the closed-loop response for the brake torques in Figure 12. As shown in Figure 12, the electro-hydraulic brake has the lowest overshoot, followed by the electromechanical brake and electronic wedge brake.

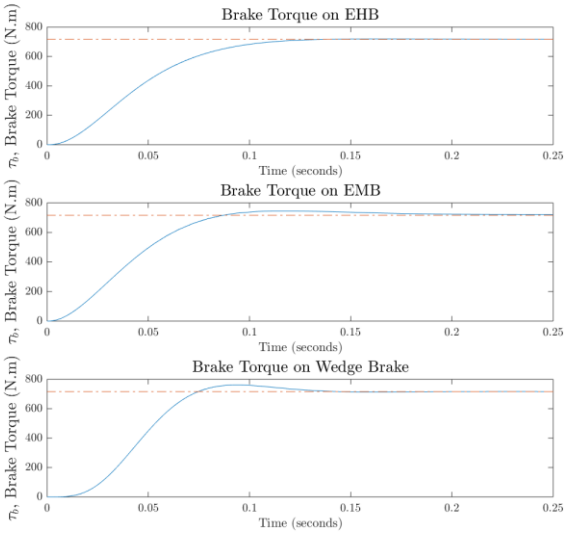

Figure 12: Closed-Loop response for each brake system – Brake Torque

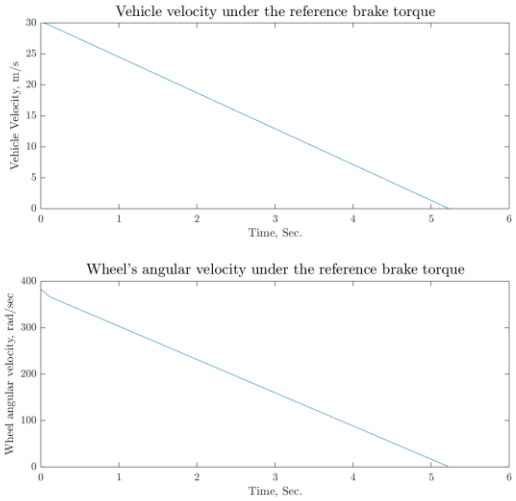

Figure 13: Vehicle velocity and wheel angular velocity under the specified brake torque reference

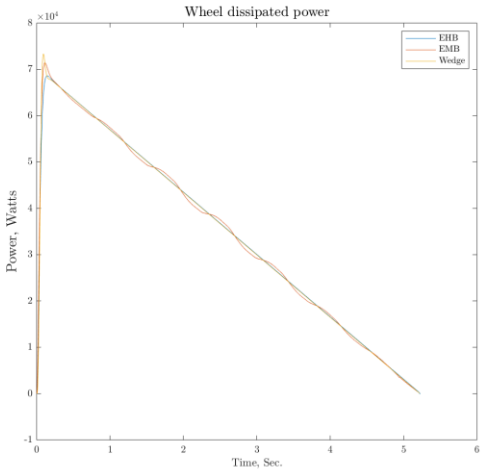

Figure 14: Dissipated Wheel Power used by each brake system under the step response in closed-loop control system

6 FUTURE WORK

For future work, a reference model for the brake torque can be added to test these brake systems under different road conditions and perform ABS maneuvers. Actuator effort and energy efficiency of the actuators is another important aspect of these actuators and their control design which is going to be evaluated under different maneuvers. Optimization of system parameters in open-loop and closed-loop is under investigation. Ultimately, a comparison of these brake systems based on different criteria will be performed.

REFERENCES

[1] Y. Yuan, J. Zhang, Y. Li, and C. Lv, "Regenerative Brake-by-Wire System Development and Hardware-In-Loop Test for Autonomous Electrified Vehicle," presented at the WCX™ 17: SAE World Congress Experience, Mar. 2017, DOI: 10.4271/2017-01-0401.

[2] P. Sinha, "Architectural design and reliability analysis of a fail-operational brake-by-wire system from ISO 26262 perspectives," *Reliab. Eng. Syst. Saf.*, vol. 96, no. 10, pp. 1349–1359, Oct. 2011, DOI: 10.1016/j.ress.2011.03.013.

[3] B. D. M. Gombert, M. Schautt, and R. P. Roberts, "The Development of Alternative Brake Systems," in *Encyclopedia of Automotive Engineering*, D. Crolla, D. E. Foster, T. Kobayashi, and N. Vaughan, Eds. Chichester, UK: John Wiley & Sons, Ltd, 2014, pp. 1–11.

[4] Bob Chabot, "Brake to the Future," *Motor*, pp. 18–24, Jun. 2015.

[5] Dirk Hofmann, Juergen Binder, Martin Pfau, Eberhardt Schunck, "HYDRAULIC BRAKE SYSTEM FOR A VEHICLE," 6,149,247.

[6] H.-J. Feigel, "Integrated Brake System without Compromises in Functionality," *ATZ*

Worldw., vol. 114, no. 7–8, pp. 46–50, Jul. 2012, doi: 10.1007/s38311-012-0192-y.

[7] J. S. Cheon, "Brake By Wire System Configuration and Functions using Front EWB (Electric Wedge Brake) and Rear EMB (Electro-Mechanical Brake) Actuators," presented at the SAE 2010 Annual Brake Colloquium And Engineering Display, Oct. 2010, doi: 10.4271/2010-01-1708.

[8] C. Line, C. Manzie, and M. Good, "Control of an Electromechanical Brake for Automotive Brake-By-Wire Systems with an Adapted Motion Control Architecture," presented at the SAE 2004 Automotive Dynamics, Stability & Controls Conference, and Exhibition, May 2004, doi: 10.4271/2004-01-2050.

[9] T. Yamasaki, M. Eguchi, and Y. Makino, "Development of an Electromechanical Brake," p. 9.

[10] C. Line, C. Manzie, and M. C. Good, "Electromechanical Brake Modeling and Control: From PI to MPC," *IEEE Trans. Control Syst. Technol.*, vol. 16, no. 3, pp. 446–457, May 2008, doi: 10.1109/TCST.2007.908200.

[11] R. Schwarz, R. Isermann, J. Böhm, J. Nell, and P. Rieth, "Modeling and Control of an Electromechanical Disk Brake," presented at the International Congress & Exposition, Feb. 1998, doi: 10.4271/980600.

[12] C. Line, C. Manzie, and M. Good, "ROBUST CONTROL OF AN AUTOMOTIVE ELECTROMECHANICAL BRAKE," *IFAC Proc. Vol.*, vol. 40, no. 10, pp. 579–586, 2007, doi: 10.3182/20070820-3-US-2918.00078.

[13] T. Sakamoto, K. Hirukawa, and T. Ohmae, "Cooperative control of full electric braking system with independently driven four wheels," in *9th IEEE International Workshop on Advanced Motion Control, 2006.*, Istanbul, Turkey, 2006, pp. 602–606, DOI: 10.1109/AMC.2006.1631728.

[14] H. Hartmann, M. Schautt, A. Pascucci, and B. Gombert, "eBrake® - The Mechatronic Wedge Brake," presented at the 20th Annual Brake Colloquium And Exhibition, Oct. 2002, pp. 2002-01–2582, DOI: 10.4271/2002-01-2582.

[15] J. Fox, R. Roberts, C. Baier-Welt, L. M. Ho, L. Lacraru, and B. Gombert, "Modeling and Control of a Single Motor Electronic Wedge Brake," presented at the SAE World Congress & Exhibition, Apr. 2007, DOI: 10.4271/2007-01-0866.

[16] K. Han, M. Kim, and K. Huh, "Modeling and control of an electronic wedge brake," *Proc. Inst. Mech. Eng. Part C J. Mech. Eng. Sci.*, vol. 226, no. 10, pp. 2440–2455, Oct. 2012, doi: 10.1177/0954406211435584.

[17] M. H. Che Hasan, M. Khair Hassan, F. Ahmad, and M. H. Marhaban, "Modelling and Design of Optimized Electronic Wedge Brake," in *2019 IEEE International Conference on Automatic Control and Intelligent Systems (I2CACIS)*, Selangor, Malaysia, Jun. 2019, pp. 189–193, DOI: 10.1109/I2CACIS.2019.8825045.

[18] J. S. Cheon, J. Kim, and J. Jeon, "New Brake By Wire Concept with Mechanical Backup," *SAE Int. J. Passeng. Cars - Mech. Syst.*, vol. 5, no. 4, pp. 1194–1198, Sep. 2012, doi: 10.4271/2012-01-1800.

[19] M. A. A. Emam, A. S. Emam, S. M. El-Demerdash, S. M. Shaban, and M. A. Mahmoud, "Performance of Automotive Self Reinforcement Brake System," *J. Mech. Eng.*, vol. 1, no. 1, p. 7, 2012.

[20] F. Ahmad, K. Hudha, S. Mazlan, H. Jamaluddin, V. Aparow, and M. M. Yunos, "Simulation and experimental investigation of vehicle braking system employing a fixed caliper based electronic wedge brake," *SIMULATION*, vol. 94, no. 4, pp. 327–340, Apr. 2018, doi: 10.1177/0037549717733805.

[21] L. M. Ho, R. Roberts, H. Hartmann, and B. Gombert, "The Electronic Wedge Brake - EWB," presented at the 24th Annual Brake Colloquium and Exhibition, Oct. 2006, doi: 10.4271/2006-01-3196.

[22] M. H. Putz, C. Wunsch, J. Morgan, M. Schiffer, and J. Brugger, "Energy and Timing Advantages of Highly Non-Linear EMB Actuation," presented at the SAE 2013 Brake

Colloquium & Exhibition - 31st Annual, Sep. 2013, doi: 10.4271/2013-01-2067.

[23] M. H. Putz, C. Wunsch, M. Schiffer, and J. Peternel, "Test Results of A Sensor-Less, Highly Nonlinear Electro-Mechanical Brake," presented at the SAE Brake Colloquium & Exhibition - 32nd Annual, Sep. 2014, doi: 10.4271/2014-01-2541.

[24] M. H. Putz, C. Wunsch, and J. Morgan, "The VE Electro-Mechanical Car Brake for Windmills (and Railways)," presented at the SAE 2012 Brake Colloquium & Exhibition - 30th Annual, Sep. 2012, doi: 10.4271/2012-01-1796.

[25] M. H. Putz, "VE Mechatronic Brake: Development and Investigations of a Simple Electro Mechanical Brake," presented at the SAE 2010 Annual Brake Colloquium And Engineering Display, Oct. 2010, doi: 10.4271/2010-01-1682.

[26] J. Yi, L. Alvarez, R. Horowitz, and C. C. de Wit, "Adaptive emergency braking control using a dynamic tire/road friction model," in *Proceedings of the 39th IEEE Conference on Decision and Control (Cat. No.00CH37187)*, Sydney, NSW, Australia, 2000, vol. 1, pp. 456–461, doi: 10.1109/CDC.2000.912806.

[27] S. Anwar, "An anti-lock braking control system for a hybrid electromagnetic/electrohydraulic brake-by-wire system," in *Proceedings of the 2004 American Control Conference*, Boston, MA, USA, 2004, pp. 2699–2704 vol.3, doi: 10.23919/ACC.2004.1383873.

[28] J. Loyola and F. Assadian, "An Investigation Into New ABS Control Strategies," *SAE Int. J. Passeng. Cars - Mech. Syst.*, vol. 9, no. 2, pp. 869–876, Apr. 2016, doi: 10.4271/2016-01-1639.

[29] A. Soltani and F. Assadian, "New Slip Control System Considering Actuator Dynamics," *SAE Int. J. Passeng. Cars - Mech. Syst.*, vol. 8, no. 2, pp. 512–520, Apr. 2015, doi: 10.4271/2015-01-0656.

[30] Burckhardt, Manfred, *Fahrwerktechnik: Radschlupf-regelsysteme*. Vogel-Verlag, Wurtzburg, 1993.

[31] C. Canudas de Wit, R. Horowitz, and P. Tsiotras, "Model-based observers for tire/road contact friction prediction," in *New Directions in nonlinear observer design*, vol. 244, H. Nijmeijer and T. I. Fossen, Eds. London: Springer London, 1999, pp. 23–42.

[32] Jonathan Loyola, "An Investigation Into New ABS Control Strategies," University of California, Davis, 2017.

[33] N. Wang and A. Kaganov, S. Code, and A. Knudtzen, "Actuating mechanism and brake assembly," WO 2005/124180 A1, Dec. 2005.

[34] D. Karnopp, "Computer Simulation of Stick-Slip Friction in Mechanical Dynamic Systems," *J. Dyn. Syst. Meas. Control*, vol. 107, no. 1, pp. 100–103, Mar. 1985, doi: 10.1115/1.3140698.

[35] Assadian, F., *MAE 272 - Theory and Design of Control Systems Class Notes*. 2015, University of California, Davis: Davis, CA.

AUTHOR BIOGRAPHIES

Ehsan Arasteh is a PhD candidate at University of California, Davis. He holds a master's degree in mechanical engineering from UC Davis and a bachelor's degree in Aerospace and Physics from Sharif University of Tech., Tehran, Iran. His research interests are vehicle dynamics, control theory and autonomous vehicles. His email address is earasteh@ucdavis.edu.

Francis Assadian is a Professor in system dynamics and control in the department of Mechanical and Aerospace Engineering at the University of California, Davis. His expertise includes vehicle dynamics, active chassis development, alternative powertrain, energy optimization, and estimation and advanced control system design. He has over 30 years of industry experience of which 17 years are in the automotive domain at companies such as Peugeot-Citroen, Ford, and Jaguar Land-Rover. His email is fassadian@ucdavis.edu.